Continental Veterinary Journal
ISSN: 3079-0212 (ONLINE)
www.cvetj.com; editor@cvetj.com

RESEARCH ARTICLE

DOI: 10.71081/cvj/2025.055

Antibacterial Efficacy of Sol-Gel Derived Fe-Doped ZnO Nanoparticles against Multidrug-Resistant *Staphylococcus aureus* and *Escherichia coli*

M. Musa Mubashar[1*], Rahmeen Ajaz[2], Aiman Aqsa[3] and Faraz Ali[2]

[1]Institute of Microbiology, University of Agriculture Faisalabad, Pakistan; [2]Faculty of Public Health, Universitas Indonesia (UI), Depok, Indonesia; [3]Faculty of Veterinary Science, Chulalongkorn University, Thailand
*Correspondence: mmmusa7672@gmail.com

ARTICLE INFO

ARTICLE HISTORY: CVJ-25-1114

Received: 24 September 2025
Revised: 10 November 2025
Accepted: 12 November 2025
Published online: 14 November 2025

Key words:
Agar well diffusion method
Antimicrobial resistance
Iron-doped zinc oxide nanoparticles
Minimum inhibitory concentration
Staphylococcus aureus
escherichia coli

ABSTRACT

Antimicrobial resistance (AMR) is a global health issue, and multidrug-resistant bacteria are causing diseases both in humans and animals. Nanoparticles can be considered as a great substitute to cater this evolving concern. In this study, the antibacterial potential of Fe-doped zinc oxide (Fe-ZnO) nanoparticles was determined which was successfully prepared by the sol gel method against *Staphylococcus aureus* and *Escherichia coli*. After synthesizing the nanoparticles, several characterization techniques such as X-ray diffraction, scanning electron microscopy, Fourier transform infrared spectroscopy (FTIR), and zeta potential were used. The structural morphology of the nanoparticles including size, shape, and structure was described in these characterization tests. *Staphylococcus aureus* is a multi-drug-resistant pathogen and was cultured from bovine mastitis milk. Similarly, *Escherichia coli* was isolated from poultry birds with colibacillosis. The antibacterial susceptibility tests were used to determine the antibacterial effect of antibiotics selected to perform this test. Afterwards, the Fe-doped ZnO nanoparticles were tested for their antibacterial activity by agar well diffusion method and minimum inhibitory concentration. The results indicated that the sol gel derived Fe-ZnO nanoparticles have great antibacterial effect against *Staphylococcus aureus* and *Escherichia coli*. Statistical analysis showed significant difference in antibacterial results of nanoparticles against the bacteria. According to this study, Fe-doped ZnO nanoparticles can be considered a potential antibiotic replacement for combating AMR.

To Cite This Article: Mubashar MM, Ajaz R, Aqsa A and Ali F, 2025. Antibacterial Efficacy of Sol-Gel Derived Fe-Doped ZnO Nanoparticles against Multidrug-Resistant *Staphylococcus aureus* and *Escherichia coli*. Continental Vet J, 5(2): 239-250. http://dx.doi.org/10.71081/cvj/2025.055

INTRODUCTION

Antimicrobial resistance (AMR) is ranked as the biggest threat by the worldwide medical community of all the challenges that influence human health, food markets and social development. According to the World Health Organization (WHO) (2020), antimicrobial resistance is included in the top ten human public health threats at the global level. These diseases can be found to have an economic impact on the magnitude of the financial crisis of 2008-2009 (O'Neill *et al.* 2016). AMR affects all types of industry, including the frequent practices of administering antibiotics to productive animal farms, such as poultry farms and the milk-producing industry (Van Boeckel *et al.* 2015). These approaches have contributed to the evolution of resistant bacteria in both animals that subsequently infect humans through close contact, environmental reservoirs and through the food chain, and are already a major One Health issue (Ahmad *et al.* 2023)

The misuse of antibiotics is a point of great concern in the third world countries, where there is no proper control measures over medicine distribution. There is also very little diagnostic and poor education of the population regarding the use of antibiotics (Brower *et al.* 2017). The continuous spread of AMR in the agricultural animal industry needs some unique and novel approaches to overcome such problems. Nanoparticles have shown great success in overcoming AMR (Moo *et al.* 2020).

It is difficult to combat bacterial diseases caused by multidrug-resistant (MDR) bacteria, such as *Escherichia coli* and *Staphylococcus aureus,* in both human and veterinary practice (Walther *et al.* 2017). There are many symptoms including skin infections, gut issues, and mastitis in cattle, goats, and sheep that is caused by

Staphylococcus aureus (Anwaar *et al.* 2023). The resistance of these bacteria reduces the efficacy of conventional antibiotics. The current sector of medicine needs new treatments that can be utilized to replace or improve existing treatments (Ventola, 2015).

Generally, most individuals tolerate *E. coli* in the intestines without any complications, but it can transform into a pathogen and cause infections such as urinary tract infections, meningitis, and other infections (Smith *et al.* 2017). The current picture includes one of the issues that many antibiotics are ineffective due to the increasing prevalence of ESBL-producing strains of *E. coli* (Naiel *et al.* 2024).

The recent literature on managing the growing pathogen resistance that is increasing and devoted to using natural compounds and developing materials as alternatives to combat resistant pathogens is extensive. The latest technique is a sinister one that pursues nanoparticles and metal-doped nanoparticles (Sharma *et al.* 2016). The nanoparticles exhibited an outstanding capacity to withstand bacterial growth. Nanoparticle technology is based on exceptional characteristics, such as a significant surface area, small size, and molecular binding capacity, which can remove microbial hazards. The introduction of Fe-NPs as an innovative material has proven to be a better antimicrobial material since the addition of iron ions not only displays antimicrobial effects but also increases both the stability of the nanoparticle and its biological behavior (Slavin *et al.* 2017).

It has been scientifically proven that the efficiency of ZnO nanoparticles increases when these structures are iron-doped, as this method leads to increased ROS production and increased cell membrane disruption in bacteria. ZnO nanoparticles with added iron decreased the viability of *S. aureus* and *E. coli* at a minimum inhibitory concentration of 10 mg/mL (Zhang *et al.* 2021).

Nanoparticle technology has emerged to be a great technique in the search for novel approaches against drug-resistant pathogens (Sharma *et al*. 2016). Nanoparticles are characterized by the combination of physicochemical properties, such as a significantly high surface-volume ratio and/or low particle size (1-100 nm) that enables them to permeabilize and destabilize bacterial cell surfaces. Nanoparticles containing defects of iron are even more virulent against bacteria (Slavin *et al*. 2017). Furthermore, studies have demonstrated that doping of ZnO with an iron ion (Fe^{3+}) result in higher stability and biological performance (Slavin *et al.* 2017). Laboratory testing has shown that a central mode of action for these nanoparticles is ROS generation (including hydroxyl radicals (OH) and superoxide anions (O2)) upon excitation with light, or on interaction with bacterial cells (Slavin *et al.* 2017). The reactive oxygen species have a destructive impact on bacterial cell membranes, proteins, and DNA, leading to bacterial cell death (Slavin *et al*. 2017).

Moreover, iron doping gives the nanoparticles the necessary magnetic characteristics to enable targeted delivery to the location of infection through the application of external magnetic fields, allowing localized treatment with a minimum number of side effects on healthy tissues (Sun *et al.* 2019). Doping enables the volume and morphological flexibility of nanoparticles, which is a potent tailored approach for designing next-generation antimicrobial agents (Chen *et al.* 2018).

Fe-doped ZnO nanoparticle was prepared by the sol-gel process, and further the structural, morphological, and surface properties of the nanoparticles were characterized by X-ray diffraction (XRD), Scanning electron microscope SEM, Fourier-infrared spectroscopy FTIR and Zeta potential analysis (Sardar *et al.* 2024). For photocatalytic breakdown of methylene blue dyestuff, UV light experiments were carried out within the control space of 60 min (Smith *et al.* 2017). It was found that the photocatalytic activity of ZnO nanoparticles was greatly enhanced after the addition of iron. High antimicrobial activity was reported because of Fe doping during antibacterial tests using Gram-negative *Escherichia coli* and Gram-positive *Staphylococcus aureus* using the disc diffusion method (Mușat *et al.* 2017). In the present study, iron doped ZnO nanoparticles were prepared by sol-gel method. Main objective of this study was to identify the antibacterial activity of Fe-ZnO nanoparticles against *S. aureus* and *E. coli* by agar well diffusion and minimum inhibitory concentration (MIC) technique.

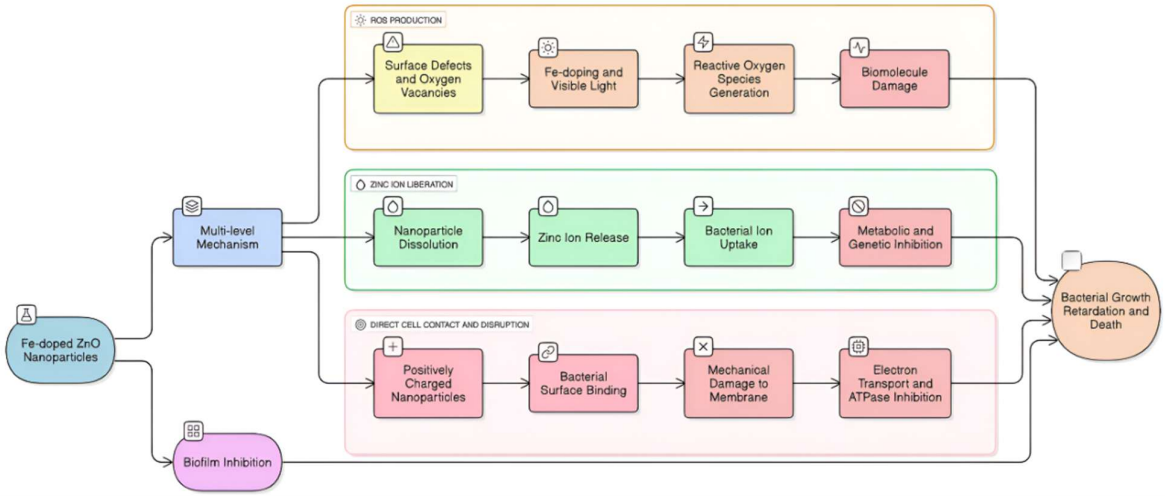

Fig. 1: Schematic Diagram of Mechanism of Action of Iron-doped Zinc Oxide Nanoparticles against bacteria.

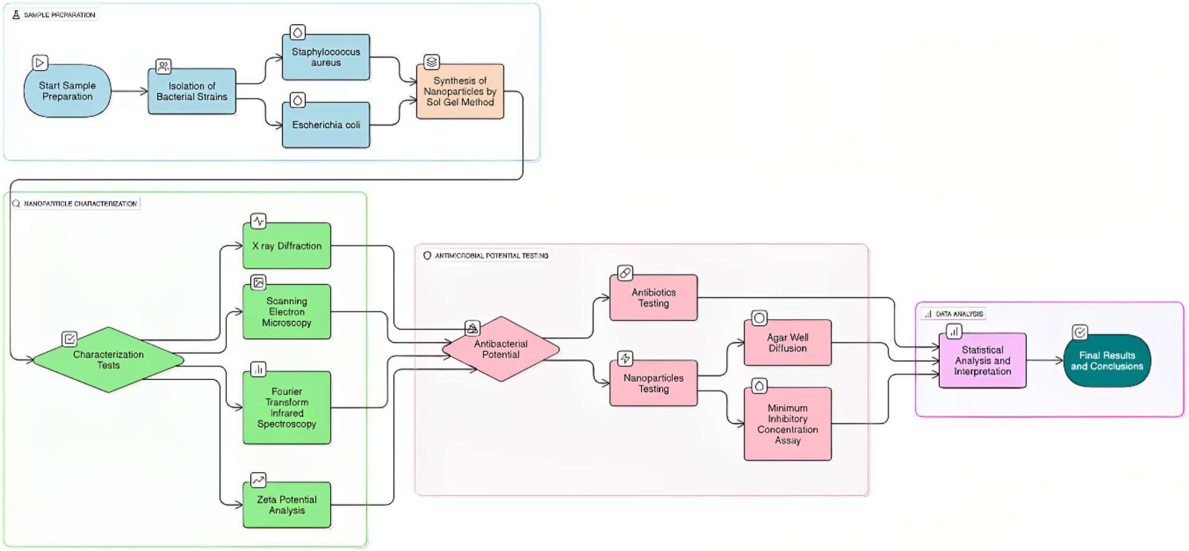

Fig. 2: Schematic Diagram of the workflow of the whole study.

MATERIAL AND METHODS

Ethical Approval

Ethical approval for data collection from animals was obtained from the Institutional Biosafety Committee of the University of Agriculture, Faisalabad. All procedures were performed following institutional bioethical standards and with the prior permission of the participating dairy farms. Various measures were adopted to safeguard the rights, dignity, and privacy of stakeholders and ensure the validity, reliability, and integrity of the data.

Isolation of *Staphylococcus aureus*

Sample Collection

A total of 40 bovine milk samples was collected from cows and buffaloes with clinical and subclinical mastitis. The samples were obtained from clinical cases at the University of Agriculture, Faisalabad, and from different farm animals. Sterile and aseptic collection was performed carefully to avoid contamination. The end of the teat was wetted with 70 percent alcohol, and initial drops of milk were discarded. Then, the samples were collected into transportable Falcon tubes.

Pre-enrichment and Isolation

Milk samples were initially inoculated in sterile nutrient broth and incubated at 37°C for 18–24 h to resuscitate bacteria, especially *Staphylococcus aureus*, as well as to enhance recovery (Glassmoyer *et al.* 2001). Isolated colonies were obtained by enrichment, followed by streaking on nutrient agar and incubating the agar at 37°C for 24 h. Further analysis was performed on colonies with typical morphology, such as round, opaque, golden, or cream-colored (Min *et al.* 2022).

Selective Isolation on Mannitol Salt Agar

To selectively differentiate, the samples were kept on Mannitol Salt Agar (MSA), which included 7.5 percent NaCl to select against non-halotolerant bacteria (Kumurya, 2017). Mannitol and phenol red were also used as pH indicators in the medium. The presence of *S. aureus* in mannitol fermentation results in a yellow hue of the medium, indicating the presence of a living organism and separating it among the staphylococci (Kumurya, 2017).

Fig. 3: Milk sample from a cow suffering from mastitis.

Microscopic and Biochemical Identification

The isotope colonies were isolated, and a sequence of tests was performed to determine the isolated colonies.

Gram Staining

A smear of bacterial culture was placed on a glass slide, a sample was heat-fixed and covered with the Gram stain technique as follows: crystal violet of Gram, both iodine of Gram and acid alcohol, and safranin of Gram. Microscopic observation under an oil immersion objective allowed the identification of atypical gram-positive and purple-staining cocci-shaped cells in clusters, which is a typical feature of *Staphylococcus aureus* (Becerra *et al.* 2016).

Biochemical Tests

Two or a mix of biochemical tests were performed to confirm the identity of the isolates. The catalase test was used to distinguish between Staphylococcus (positive) and Streptococcus (negative). A coagulase test was conducted to determine the presence of the enzyme coagulase, which clots plasma and is one of the main distinguishing hallmarks of *S. aureus* (Sperber *et al.* 1975). A Voges-Proskauer (VP) reaction was performed to probe the fermentation of glucose to acetoin in the Voges-Proskauer (VP) reaction; a positive reaction confirmed the presence of *S. aureus*. Finally, the citrate test was conducted to determine whether the organism could utilize citrate as the only carbon source (Van Hofwegen *et al.* 2016).

Isolation of *Escherichia coli*

Sample Collection

Forty liver samples of poultry (broilers and layers) suspected of having colibacillosis were collected for the isolation of *Escherichia coli*. These small samples were collected from a few poultry farms and the Diagnostic Pathology Laboratory of the University of Agriculture, Faisalabad. Strict adherence to aseptic procedures was considered during dissection and sample collection to prevent cross-contamination. Liver tissue was preserved neatly in ice-cooled sterile vessels and taken to the laboratory to undergo analysis. All samples were carefully marked with their origin and identification number so that they could be traced carefully.

Fig. 4: Taking *E. coli* samples from poultry liver.

Pre-enrichment and isolation

Samples were pre-enriched in Brain Heart Infusion (BHI) at 37°C for 24 h. After inoculation, the broth became viscous, which affected the results as a sign of bacterial growth and the presence of viable chambers. The cultures were then aseptically streaked onto MacConkey Agar, a selective and differential culture medium that supports gram-negative bacteria and distinguishes between lactose fermenters and non-fermenters. *E. coli* was confirmed on the chicken liver because of pink colonies that resulted when lactose was fermented. Microscopic and Chemical Identification. Isolates were Gram-stained, which confirmed Gram-negative populations consisting of pink rod-shaped bacilli, suggesting the initial identification of *E. coli* (Becerra *et al.* 2016). For unambiguous confirmation, conventional IMViC biochemical tests were performed. *E. coli* was positive for Indole (tryptophan metabolism) and positive for Methyl Red (MR) (acid produced by glucose fermentation and stable). Non-acidic metabolites were not detected in the Voges–Proskauer (VP) procedure, and the inability to utilize citrate as the sole source of carbon was detected in the citrate test. The classical IMViC profile (synergistic- (++) characteristic with antagonistic (mandelic acid- (formolic acid)) confirmed the identities of the isolates as *E. coli* (Van Hofwegen *et al.* 2016).

Antimicrobial Susceptibility Testing (AST)

The antibiotic susceptibility of the identified bacterial isolates was measured using the Kirby-Bauer disk diffusion method according to Clinical and Laboratory Standards Institute (CLSI) (Graham *et al.* 1985). The growth medium used was Mueller-Hinton agar (MHA) due to the non-selective and non-differentiating characteristics which can ensure maximum growth of bacteria along with diffusion of the antibiotics (Zakir *et al.* 2021; Kollerup *et al.* 2022). A suspension of this bacterium was made and diluted to 0.5 McFarland standard (~1-2 × 10^8 CFU/ml). The MHA plates that were inoculated with the bacteria were then inserted with sterile antibiotic disks and incubated at 37°C for 24 h. Susceptibility or resistance of the bacteria strains to the antibiotics was measured using the diameter of zone of inhibition around each disk in millimeters.

Preparation and Characterization of Iron-Doped Zinc Oxide Nanoparticles

Synthesis

Fe-ZnO nanoparticles with iron doping were prepared using a normal sol-gel procedure (Musat *et al.* 2017). The synthesis process was carried out by mixing zinc sulfate ($ZnSO_4$) and iron sulfate ($FeSO_4$) cautiously as the materials. A 1 M solution of $ZnSO_4$ was prepared by dissolving $ZnSO_4 \cdot 7H_2O$ in distilled water independently, and a 1 M solution of $FeSO_4$ was prepared separately using $FeSO_4 \cdot 7H_2O$. The precipitating agent used was a 1 M sodium hydroxide solution. Zinc sulfate solution (95 mL) was first stirred, as shown in Figure 3, which shows that the doping percentage decreased during the addition of further titrants into the mixture and peaked at 9000 rpm, thus illustrating that 2.5 mol of doping was reached. Sodium hydroxide was added dropwise until the pH was brought to the 10-11 range, which resulted in light precipitate formation. The mixture was then stirred. To achieve full gelation, the mixture was maintained for 1–2 h and then left for 12–24 h to age. The resulting precipitate was washed with distilled water and ethanol several times to remove impurities, dried in a hot air oven at 80-100°C for 12 h, and ground into a fine powder. The resultant product was heated at 400–500°C for 2-3hours in a muffle furnace to obtain the required particle structure.

Table 1: Composition of Fe-ZnO Nanoparticles (for 100 mL total metal ion solution)

Component	Concentration	Volume Used	Purpose
Zinc	1 M	95 mL	Zinc precursor
Iron	1 M	5 mL	Iron dopant (5 mol%)
Sodium hydroxide	1 M	~100 mL	Precipitating agent
Distilled water	—	As needed	Dilution and washing
Ethanol	—	As needed	Washing agent

Characterization
A variety of techniques were used to identify the structure and morphology of the synthesized nanoparticles (Sardar *et al.* 2024).

X-Ray Diffraction (XRD): XRD technique was used to identify the crystalline structure of the nanoparticles. This was done to ensure that the crystal structure is of the hexagonal type of wurtzite and that the iron is in the lattice of the zinc oxide phase (Rao *et al.* 2023).

Scanning Electron Microscope (SEM): The morphology and size of the synthesized nanoparticles were examined by Scanning Electron Microscope (SEM) (Sardar, *et al.* 2024). The method gave a clear image of the shape of the particles and how they aggregated.

Fourier Transform Infrared Spectroscopy (FTIR): Fourier Transform Infrared Spectroscopy was performed for the determination of the functional groups and chemical bonds, that are present on the surface of the nanoparticles (Pasieczna-Patkowska *et al.* 2025). It refuted the presence of other typical bonds, like ZnO, and gave evidence of the other sample's purity.

Zeta Potential Analysis: Zeta potential of the nanoparticles was performed to find out the surface charge present on the nanoparticles. This parameter is very important as it ensures the proper measurement of the particle's stability and bacterial cell interactions.

Antibacterial Efficacy Testing
Agar Well Diffusion Method
The antibacterial potential of Fe-ZnO nanoparticles were measured using the Agar Well Diffusion method. *S. aureus* and *E. coli* were inoculated or streaked on the plate containing the Mueller-Hinton agar (Murray *et al*. 1983). Wells were made that has diameter of almost 6-7 mm. These wells were scraped on the agar using a sterile instrument. After that, 50-100 mL of a nanoparticle suspension of 1 mg/mL was added in each well. The plates were then incubated for 18 to 24 h after to the inoculation of the nanoparticle's suspension. A zone of inhibition in millimetres (mm), was measured around each well, as a measure of the antibacterial effect (Holder *et al.*1994).

Minimum Inhibitory Concentration (MIC)
The Minimum Inhibitory Concentration (MIC) assay was performed to identify the lowest concentration of the nanoparticles which is sufficient to prevent the growth of bacteria. It was done through serial dilution in two-steps (Vassallo *et al*. 2018). Known dilutions of the nanoparticle suspensions were made in sterile broth to generate a concentration gradient of nanoparticle suspensions. A typical bacterial inoculum is in the order of 10^5 to 10^6 CFU/mL (Montville *et al.* 2003).
Then each well was inoculated with 10^6 CFU/mL. After incubation the wells spanned 18-24 hours at 37°C (approx.). After incubation, all wells were examined visually for turbid versus non-turbid, representing mucoid versus non-mucoid bacterial growth (culture). From this calculation, the total concentration of the suspension of nanoparticles without detectable bacterial growth was defined as the MIC. In addition to this, the optical density (OD) of each well were defined at 620 nm by spectrophotometer; the lower the OD, the lower the bacterial growth and the deeper the antibacterial response (Parvekar *et al.* 2020).

RESULTS

Isolation of Bacterial Strains
Isolation of *Staphylococcus aureus*
In Faisalabad, 40 milk samples were taken for bovine mastitis throughout different dairy farms and at the University of Agriculture, Faisalabad. The identification and confirmation of *Staphylococcus aureus* using a set of enrichment, isolation, and biochemical assays were automated on the samples processed and cultured.

Growth of *S. aureus*
Samples were inoculated in nutrient broth (NB) and streaked on Nutrient agar, and colonies of *S. aureus* morphology (iconic, opacity, round, golden/cream color) were selected. These were purified on Mannitol Salt Agar, where mannitol-fermenting isolates turned the phenol red indicator to yellow and presumptively identified as *S. aureus*.

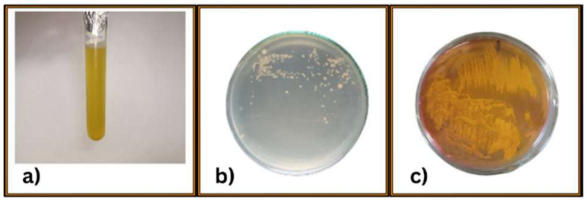

Fig. 5: Growth of *Staphylococcus aureus* on different media: a) Growth of *Staphylococcus aureus* on nutrient broth, b) Growth of *Staphylococcus aureus* on Nutrient Agar, c) Growth of *Staphylococcus aureus* on Mannitol Salt Agar.

Gram Staining
The presumptive isolates were followed by Gram staining to conclusively identify them. Gram staining was used to confirm the existence of Gram-positive cocci in grape-like clusters, one of the main morphological features of *S. aureus*.

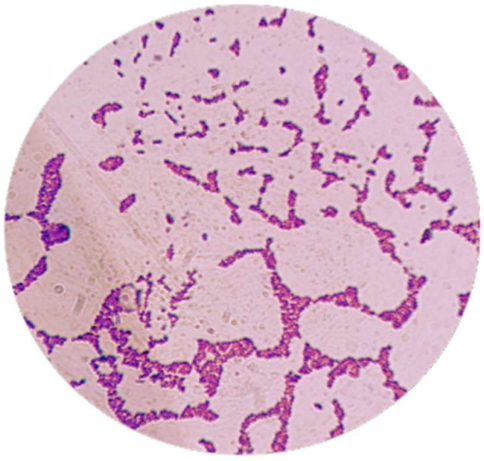

Fig. 6: Gram staining of *S. aureus.*

Biochemical tests of *S. aureus*

Catalase Test: Thirty-five of the isolates tested positive with respect to catalase enzyme, and 5 were negative.

Coagulase Test: Thirty-five of the isolates were positive regarding the production of coagulase, with five of them giving a negative result.

Voges-Proskauer Test: A total of thirty-four were positive concerning the production of acetoin, and six were negative.

Citrate Utilization Test: Thirty-six of them were positive, demonstrating that they could utilize citrate as their only carbon source; four of them were negative.

Through the overall outcome of all these biochemical tests, each of the 40 samples was finally determined. *Staphylococcus aureus* was positive in 21 samples and negative in 19 samples.

Through the overall outcome of all these biochemical tests, each of the 40 samples was finally determined. *Staphylococcus aureus* was positive in 21 samples and negative in 19 samples.

Isolation of *Escherichia coli*

Isolation and Growth

Forty samples were sampled and pre-cultured in the brain heart infusion (BHI) broth, and the turbidity in the broth was an indicator of bacterial growth. Following pre-enrichment, MacConkey agar plates, which are developed to take care of Gram-negative bacteria that ferment lactose, were isolated with the samples. *E. coli* colonies grew pink with lactose fermentation because the same acid generated that reacts with the neutral red pH test reagent in the medium. This was to test the presence of the bacteria in the sample.

Gram Staining Identification

Isolated *E. coli* was prepared by measuring Gram staining and thereafter subjected to a range of biochemical tests. It was revealed that Gram-negative, pink-stained, rod-shaped bacilli were found either individually or in small groups with Gram-stained reagents.

The following were the biochemical test results:

Indole Test

28 isolates detected a positive antigen as they produced a red or pink zone, as shown by the formation of the red/pink color following the addition of the reagent (Kovac).

Methyl Red Test

26 isolates were positive regarding the production of acetyl carbinol.

Voges-Proskauer Test

26 isolates were negative in terms of the absence of metabolite production of non-acidic ones.

Test of the Citrate

29 isolates had a negative result in terms of citrate use since *E. coli* does not usually produce the required enzyme.

Using the combined outcomes of these tests, 25 *Escherichia coli* positive isolates were determined, and 15 *Escherichia coli* negative isolates were determined.

Antimicrobial Susceptibility Testing

AST on *S. aureus*

Antimicrobial susceptibility testing was done on *S. aureus* with different antibiotics using the disk diffusion method. The results showed that this bacterium was resistant to antibiotics, including ceftazidime and amoxicillin. However, doxycycline, erythromycin, and lincomycin have shown great antibacterial potential against these bacteria. The one-way ANOVA showed that the mean zone of inhibition and standard deviation among different antibiotics against *S. aureus* shows extreme low p value which is $P < 0.0001$. It indicates that at least one of the antibiotics shows significantly different results which reject the null hypothesis.

AST on *E. coli*

AST was also done on *E. coli* with a similar disk diffusion method. The results showed great resistance of *E. coli* against commonly used antibiotics like amoxicillin, doxycycline, and erythromycin. However, norfloxacin, colistin, and ceftazidime showed good results. The one-way ANOVA showed that the mean zone of inhibition and standard deviation among different antibiotics against *E. coli* shows extreme low p value which is $P < 0.0001$. It indicates that at least one of the antibiotics shows significantly different results which reject the null hypothesis.

Characterization of Fe-ZnO Nanoparticles

X-Ray Diffraction XRD Results

ZnO was identified to contain a crystal structure of hexagonal wurtzite. The analysis by X-ray diffraction showed that the (100), (002), and (101) planes had the same diffraction peaks as the known ZnO (JCPDS 36-1451). The peaks of homogenized doped ZnO in the same planes (100) (002) are shorter than those found in zinc acetate/sodium hydroxide ZnO. In the case of (101), the peak has become narrower and sharper, is taller and reflects smaller, more

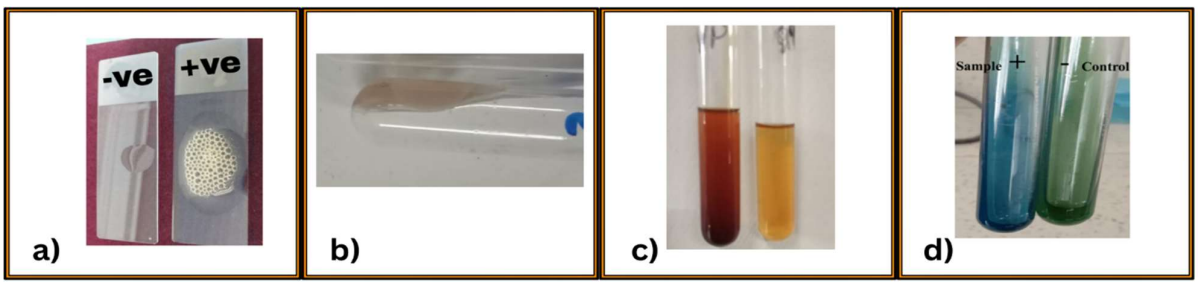

Fig. 7: Biochemical test results of *S. aureus*, (a) Catalase test results, bubble formation show a positive result, (b) Coagulase test, in which clothing shows a positive result, (c) Voges-Proskauer result shows a positive result by production of acetoin, (d) Citrate utilization test, which shows how citrate can be used as a carbon source.

uniform crystallites. Although ZnO has been doped with ferric ions, the major peak observed under 36.275° (2θ) is changed slightly, and no other ferric oxide peak is observed, which proves that ZnO still belongs to the crystalline structure. Due to the variation in FWHM, the crystallite size was calculated as 20. 37 nm, and the structure of doped ZnO did not correspond to what was assumed undoped ZnO was supposed to look like.

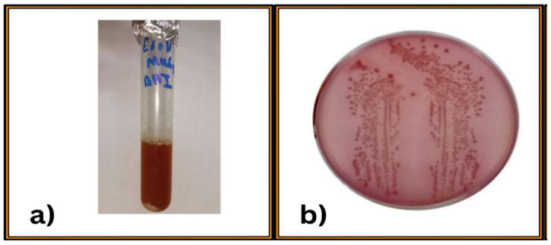

Fig. 8: Growth of *E. coli* on different media, (a) growth of *E. coli* on Brain Heart Infusion Broth, (b) Growth of *E. coli* on MacConkey Agar showing pink color colonies.

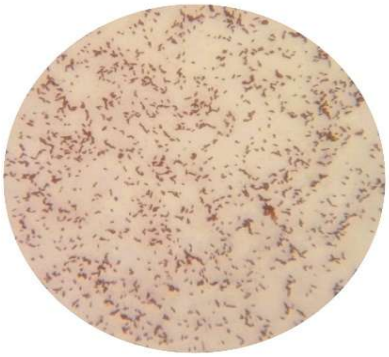

Fig. 9: Gram staining of *E. coli.*

Scanning Electron Microscope

Nano-flake Iron-doped ZnO was prepared as opposed to a nanospherical shape in the micrograph at 20 KX. In the micrograph, you can more easily visualize the shape and the sizes of the flakes in the nanoflakes. The flakes were attracted out of the agglomerate due to their polar and highly charged flat surfaces. The particles composing each flake are 100x70 nm in radius, and the thickness of the flake is average in the range of 20 to 25nm. Post-doping ZnO with ferric ions provided nanostructures of thin thickness and morphologies compared to those before.

Fourier Transform Infrared Spectroscopy FTIR Results

FTIR-based analysis provided information about the surface existence of -OH groups on the composite. The spectra obtained in Fe-ZnO samples are shown in (Fig. 4.17). The FTIR established the presence of the species, iron, and zinc, as well as confirmed the locality of the functional groups and structures of the functional groups in 2.51% of iron in iron-zinc oxide. Recombination of the OH groups was the cause of reducing this band. In addition to the foregoing, there appears to be a cracked peak in 3860.67 cm−1, indicating that a certain amount of water had been incorporated into the folds of the polysaccharide, and the low peak in the range of 1096.55 cm−1, indicating the presence of the C-O bond stretch belonging to the carbonoxyl group of glucose in the fibres. No appearance of carbon-based functional groups in the sample was observed by the absence of any peaks at the positions of 1500-1650 cm−1 and 2150-2350 cm−1. And it implies that Fe-ZnO is highly pure according to the norms. The action of Fe influenced the structural characteristics of ZnO, where there was a small peak at 510.45 cm−1. No band was observed below 500 cm−1 corresponding to the Zn-O band of undoped ZnO, but was rather shifted and found not at a lower frequency, but at a higher frequency, 535 cm−1in the Fe-doped ZnO.

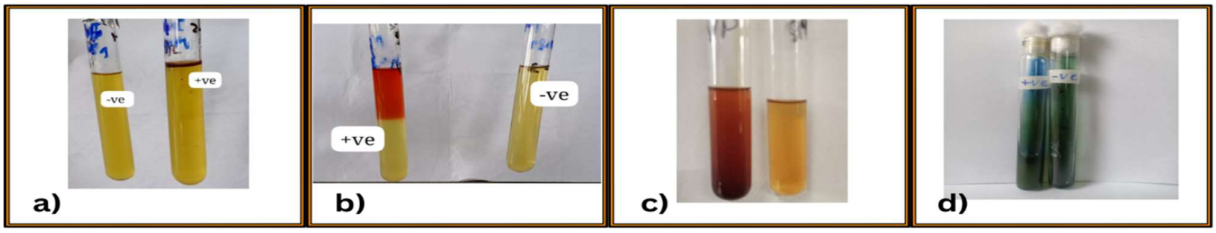

Fig. 10: Biochemical test results of *E. coli*, (a) Indole test results, red color ring shows positive result, (b) Methyl Red test in which production of acetyl carbinol shows positive result, (c) Voges Proskauer result show positive result by production of acetoin but it is negative in this case, (d) Citrate utilization test which shows how citrate can use citrate as carbon source, it is negative in this case.

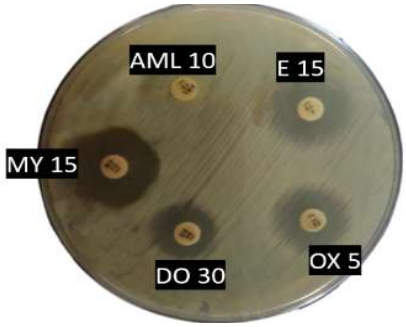

Fig. 11: AST results on *S. aureus* using the Disk Diffusion method

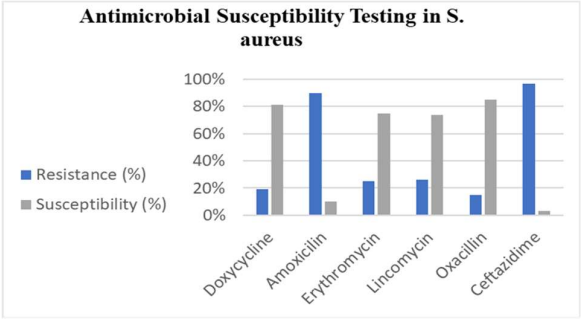

Fig. 12: AST results Graph on *S. aureus* using the Disk Diffusion method

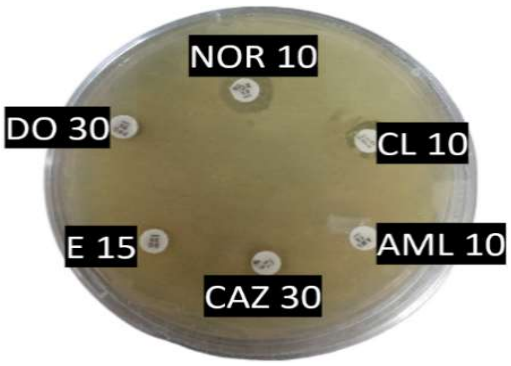

Fig. 13: AST on *E. coli.*

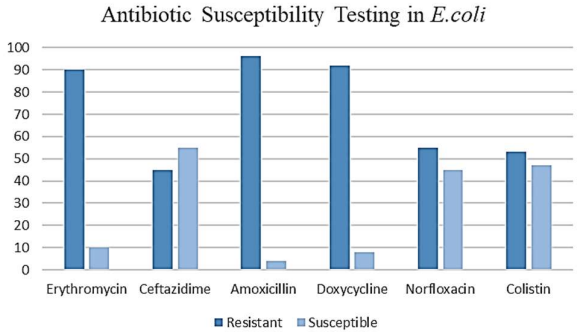

Fig. 14: Graph of AST of *E. coli.*

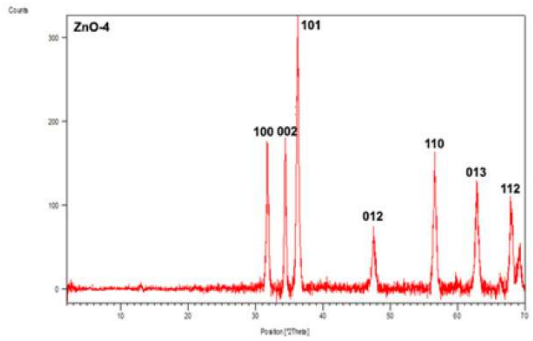

Fig. 15: XRD Results of Fe Doped ZnO Nanoparticles.

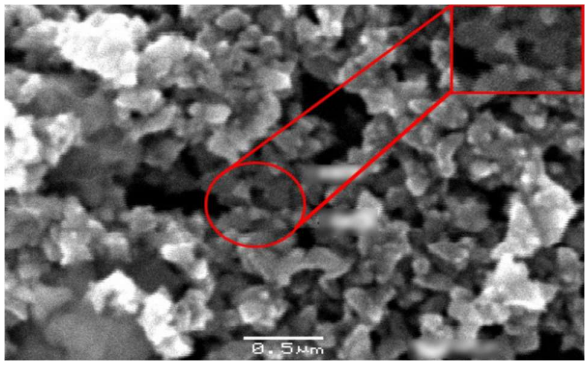

Fig. 16: SEM Results of Fe-ZnO NPs.

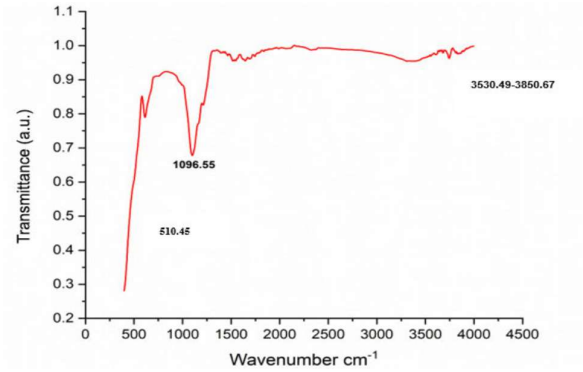

Fig. 17: FTIR Results of Fe-ZnO NPs.

Zeta Potential Results

A tremendous jump in the positive zeta potential of Fe ZnO at a specific value is recorded, which is 17.4 mV. The results of the Zeta potential indicated that the surface of every observed Fe ZnO molecule was positively charged. Since this peak moved toward the higher end, they could establish that doping I to Fe ZnO caused its zeta potential to be not equal to that of ZnO. Based on its Conductivity (1.65mS/cm) value of Fe ZnO, the photocatalyst would perform well.

Antibacterial effects of Iron Doped Zinc Oxide Nanoparticles

The Agar Well Diffusion method was used.

The use of the agar well diffusion method was also applied in this study to determine the antibacterial effects that were caused by the nanoparticles. The basic outcome of Fe-ZnO nanoparticles in the agar well diffusion method was immense intermediate. These NPs demonstrated relatively greater performance compared to *Staphylococcus aureus* when compared to *Escherichia coli*. The average diameter of inhibitory areas created by these nanoparticles siblings against the *Staphylococcus aureus* was 18.22 mm compared to the average diameter of inhibitory areas against the *Escherichia coli* at 12.33 mm.

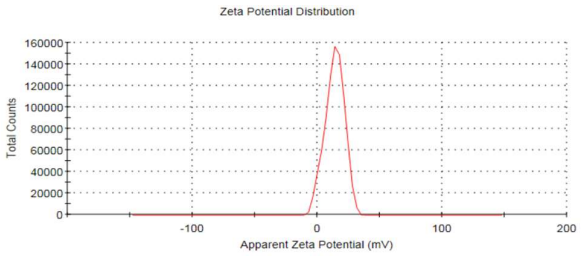

Fig. 18: Zeta Potential Results.

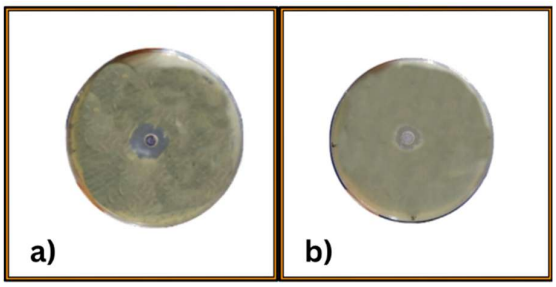

Fig. 19: Agar well diffusion method results of Fe-ZnO nanoparticles ZOI, a) Antibacterial result against *S. aureus* b) Antibacterial result against *E. coli*

Table 4: Fe-ZnO against *S. aureus* and *E. coli*

Bacteria	Mean + Standard Deviation Results (mm)
Staphylococcus aureus	18.22 ± 1
Escherichia coli	12.33 ± 0.58

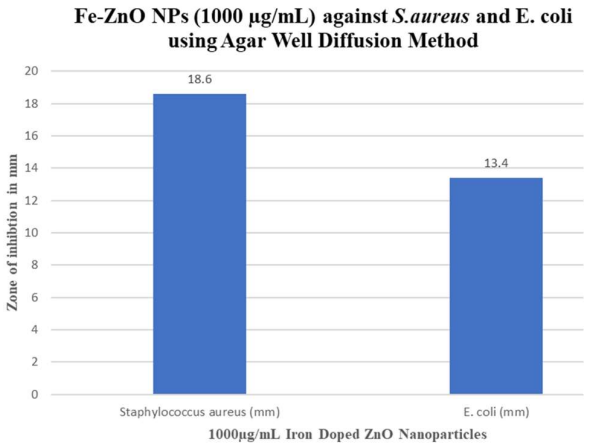

Fig. 20: Graph displaying the antibacterial effect of Nanoparticles against the bacteria.

A one-way ANOVA test was done to check the significance and the results shows that there is a significant difference between the results so the $p < 0.0001$ which means that there is a significant difference between the antibacterial results of these nanoparticles against these two bacteria.

Minimum inhibitory concentration

The minimum inhibitory concentration was also performed in this study to test the minimum dose of nanoparticles to inhibit the growth of nanoparticles and that of such bacteria.

The MIC value was also at the 2nd well, *S. aureus*. It indicates that the nanoparticles' MIC value was 500 µg/ml, and it was 250 µg/ml in *E. coli*.

Bacteria	Mean + Standard Deviation Results (mm)
Staphylococcus aureus	18.22 ± 1
Escherichia coli	12.33 ± 0.58

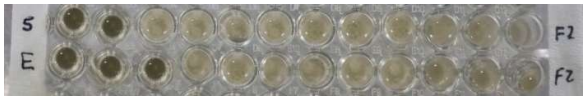

Fig. 21: Result of MIC of Fe-ZnO nanoparticles against both bacteria.

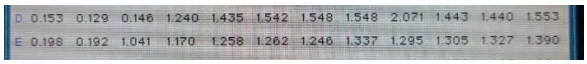

Fig. 22: OD values of MIC of Fe-ZnO nanoparticles against both bacteria in the spectrophotometer.

Nanoparticles were 500 µg/ml, whereas in *E. coli* the MIC value was 250 µg/ml.

The value was measured in the spectrophotometer, which reported the value of optical density.

The ANOVA results show that there is a significant difference in the mean values of the MIC of these nanoparticles against these bacteria. The P value obtained is less than 0.001 which means ($P<0.001$). So, statistically there is significance difference recorded.

DISCUSSION

The global rise of antimicrobial resistance (AMR) highlights an important issue to the public health, that enables the researchers to find out some novel antimicrobial agents (WHO, 2020). This study reports the successful synthesis and shows great antibacterial efficacy of iron-doped zinc oxide (Fe-ZnO) nanoparticles against multidrug-resistant (MDR) strains of *Staphylococcus aureus* and *Escherichia coli*. The results are analyzed in the context of already established literature, which also highlights the mechanisms of action and shows the potential of Fe-ZnO nanoparticles as a great substitute to conventional antibiotics.

In this study, Fe-ZnO NPs were synthesized via the sol-gel method. Broad and intense peaks were obtained from the X-ray diffraction (XRD) which highlighted a fine crystalline structure with low crystalline degree. This kind of structure is more common for sol-gel process at a low temperature (Muşat *et al.* 2017). Fourier-transform infrared (FTIR) spectroscopy was performed to verify that Fe was embedded in the ZnO lattice by a change in vibrational bands. In fact, the experiments have validated the iron doping could enhance the antimicrobial and photocatalytic activity of ZnO. In the current work, the localized surface defect and band gap modulation has been achieved (Zhang *et al.* 2021).

In terms of antibacterial activity of Fe-ZnO nanoparticles against MDR strains of *S. aureus* and *E. coli*, our results resemble to the already published studies. One of the most important findings of this study is the differential susceptibility of bacterial species, with differential vulnerability of the Gram-positive *S. aureus* and less vulnerability of the Gram-negative *E. coli*. This observation is directly correlated with the work of Yin *et al*. (2024), who likewise reported a superior effect of Fe-doped ZnO against *S. aureus* than *E. coli*. It is illustrated by the difference in the bacterial cell wall structure. Our observations further resemble by the work of Zhang *et al*. (2021), who found that iron doped ZnO nanoparticles are remarkably effective, and the major cause of enhanced activity is present in the generation of reactive oxygen species (ROS). The values obtained from the MIC in this study are similar to and even higher than those studies (Zhang *et al.* 2021; Musat *et al.* 2017; Sardar *et al.* 2024).

Though our findings follow the most recent work, it is important to acknowledge disagreements in the literature, which highlight the complexity involved in nanoparticle-based antimicrobials. In addition, although the work of Zakir *et al*. (2021) is not directly comparable with ours, since their results on emerging trends of drug-resistant bacteria in clinical facilities strengthen the importance of our research overall, as well as that of the novel agents such as those we have developed.

The mechanism of the bacterial antagonistic activity of the Fe-ZnO nanoparticles is considered to predominantly be due to the formation of reactive oxygen species (ROS), especially the hydrogen peroxide radical. An increased quantity of these highly active radicals is generated because of the ensuing boosted photocatalytic activity of the Fe-

doped ZnO (Giram *et al.* 2024). The ROS then can trigger oxidative stress, leading to lipid peroxidation of the bacterial cell membrane, disorganized cell membrane, cytoplasmic leakage and eventually to cell death (Yang *et al.* 2018). The higher susceptibility of *S. aureus* is postulated to be due to the greater permeability of its cell wall, which enables the accumulation of a higher concentration of ROS at the cell membrane and extensive damage.

The activity of synthesized nanoparticles against bacteria was tested through the antibacterial efficacy study under Agar Well diffusion, and MIC revealed the high antimicrobial action of the developed nanoparticles molecules. However, a closer look at the data reveals an interesting phenomenon. Where the nanoparticles exhibited a higher inhibition zone with *S. aureus* (18.22 mm) than *E. coli* (12.33 mm), the MIC value was lower with *E. coli* (250 mg/mL) than that of *S. aureus* (500 mg/mL). This inner paradox is attributable to the divergence between the diffusion of the antimicrobial agent in the agar and its own potency at the cellular level (Emami-Karvani and Chehrazi, 2011). A zone of inhibition depends on both the agent's efficacy and diffusion of the agent through the medium. The variation implies that a lower nanoparticle concentration is required to prevent the growth of *E. coli* (lower MIC), but the nanoparticles can diffuse less into the agar than their lethality would indicate. On the other hand, the bigger size of the inhibition zone in *S. aureus* can be attributed to faster or effective local action at the well, possibly associated with the specific wall structure. The thick cell wall of Gram-positive bacteria may be more vulnerable to physical disruption by the nanoparticles, whereas the outer membrane of Gram-negative, *E. coli*, may constitute an early diffusion barrier, though its intracellular organisms may prove more vulnerable at lower concentrations, once the barrier is crossed (Zgurskaya *et al.* 2020).

The research demonstrates sound scientific and empirical data on using iron-doped zinc oxide nanoparticles as a potential and effective antimicrobial alternative (Moo *et al.* 2020). Their great relative effectiveness asking the so-called drug-resistant pathogens, even when the sources were extremely important in the agriculture industry, testifies to their high ability as an efficient weapon in the arsenal in combating the drug-resistant pathogens. Conjunctive attention to veterinary isolates is especially topical because it directly refers to one of the main carriers of AMR transmission in the One Health approach (Velazquez-Meza *et al.* 2022). The results indicate that such nanoparticles could be optimized into a powerful therapeutic tool in animal medicine as well as, possibly, in human medicine. Further studies are needed on in vivo studies that would determine the biocompatibility of their materials in animal models. Optimization of synthesis parameters further, or optimization of the induction of homogenized nanoparticles of definite properties in cultured cells, could subsequently be studied to refine nanoparticle characteristics to a particular application and enhance their stability and sustained effectiveness.

Conclusion

The study proves the fact of a widespread multidrug resistance to *Staphylococcus aureus* and *Escherichia coli* in the local agricultural context, and it is noteworthy that the problem of antimicrobial resistance gained such widespread spread widely. The paper has managed to generate and characterize iron-doped zinc oxide nanoparticles, which showed strong antibacterial effectivity against these pathogens that are very resistant. The characterization data displayed a distinct nano-flake morphology and a preferential positive charge on the surface, and these play a part in determining the efficacy of the nanoparticles by maximizing physical as well as chemical interactions between the nanoparticles and the bacterial cell membrane. Quantitative results obtained during the Agar Well Diffusion and the MIC assays are strong indicators that these nanoparticles make a useful antimicrobial agent. This research confirms the enormous potential of nanoparticles as a new treatment mode, giving a new and promising opportunity to face antimicrobial resistance and protect human health.

DECLARATION

Funding: No funds were received for this study from any national or international funding agency.

Acknowledgement: None.

Conflicts of Interest: All the authors have no personal or financial interests.

Availability of Data and Material: All the data is included in this manuscript and may be obtained from the corresponding author.

Ethics Statement: This study was conducted following the guidelines regarding welfare and use of study animals for research purposes.

Authors Contribution: MMM: Conceptualization, Methodology, Resources, Validation, Visualization, Data curation Software, Writing-original draft. Formal analysis, AA, AR and AF; Writing-original draft, Writing-review and editing.

Generative AI Statement: The authors declare that no Gen AI/DeepSeek was used in the writing/creation of this manuscript. Publisher's Note: All claims stated in this article are exclusively those of the authors and do not necessarily represent those of their affiliated organizations or those of the publisher, the editors, and the reviewers. Any product that may be evaluated/assessed in this article or claimed by its manufacturer is not guaranteed or endorsed by the publisher/editors.

REFERENCES

Ahmad N, Joji RM and Shahid M, 2023. Evolution and implementation of one health to control the dissemination of antibiotic-resistant bacteria and resistance genes: A review. Frontiers in Cellular and Infection Microbiology 12: 1065796. DOI: 10.3389/fcimb.2022.1065796

Anwaar F, Ijaz M, Rasheed H, Shah SFA, Haider SAR and Sabir MJ, 2023. Evidence and molecular characterization of multidrug-resistant Staphylococcus aureus isolated from

equines in Pakistan. Journal of Equine Veterinary Science 126: 104498. DOI: 10.1016/j.jevs.2023.104498

Becerra SC, Roy DC, Sanchez CJ, Dziadek MM and Rumbaugh KP, 2016. An optimized staining technique for the detection of Gram positive and Gram-negative bacteria within tissue. BMC Research Notes 9: 216. DOI: 10.1186/s13104-016-1902-0

Brower CH, Mandal S, Hayer S, Sran M, Zehra A, Patel SJ and Laxminarayan R, 2017. The prevalence of extended-spectrum beta-lactamase-producing multidrug-resistant Escherichia coli in poultry chickens and variation according to farming practices in Punjab, India. Environmental Health Perspectives 125(7): 077015. DOI: 10.1289/EHP292

Chen Y, Shen Z and Du X, 2018. Surface functionalization and bioactivity enhancement of iron-doped zinc oxide nanoparticles for antimicrobial applications. Materials Science and Engineering: C 88: 16-24.

Emami-Karvani Z and Chehrazi P, 2011. Antibacterial activity of ZnO nanoparticle on gram-positive and gram-negative bacteria. African Journal of Microbiology Research 5(11): 1368-1373. DOI: 10.5897/AJMR10.159

Giram D and Das A, 2024. Synthesis and characterization of Fe doped ZnO nanoparticles for the photocatalytic degradation of Eriochrome Black-T dye. Indian Journal of Chemical Technology (IJCT) 31(1): 39-43. DOI: 10.56042/ijct.v31i1.4985

Glassmoyer KE and Russell SM, 2001. Evaluation of a selective broth for detection of Staphylococcus aureus using impedance microbiology. Journal of Food Protection 64(1): 44-50. DOI: 10.4315/0362-028x-64.1.44

Graham DR, Dixon RE, Hughes JM and Thornsberry C, 1985. Disk diffusion antimicrobial susceptibility testing for clinical and epidemiologic purposes. American Journal of Infection Control 13(5): 241-249. DOI: 10.1016/0196-6553(85)90024-0

Holder IA and Boyce ST, 1994. Agar well diffusion assay testing of bacterial susceptibility to various antimicrobials in concentrations non-toxic for human cells in culture. Burns 20(5): 426-429. DOI: 10.1016/0305-4179(94)90035-3

Islam S, Islam MA, Sultana S, et al. 2025. Exploring the Interconnectedness of E. coli Antimicrobial Resistance in Poultry, Human Health, and Environmental Factors in Bangladesh: A Review. Egyptian Journal of Veterinary Sciences 1-15. DOI: 10.21608/ejvs.2025.384337.2841

Kashif M, Al-Douri Y, Hashim U, Ali ME, Ali SMU and Willander M, 2012. Characterisation, analysis and optical properties of nanostructure ZnO using the sol–gel method. Micro and Nano Letters 7(2): 163-167. https://doi.org/10.1049/mnl.2011.0681

Kollerup I, Thomsen AKA, Kornum JB, Paulsen KI, Bjerrum L, and Hansen MP. (2022). Use and quality of point-of-care microscopy, urine culture and susceptibility testing for urinalysis in general practice. Scandinavian Journal of Primary Health Care 40(1): 3–10. DOI: 10.1080/02813432.2021.2022349

Kumurya AS. (2017). Use of Mannitol Salt Agar (MSA) and cefoxitin as a selective culture medium for growing MRSA strains. Frontiers in Biomedical Sciences 2(1): 1–5.

Maalik A, Shahzad A, Iftikhar A, Rizwan M, Ahmad H and Khan I. (2019). Prevalence and antibiotic resistance of Staphylococcus aureus and risk factors for bovine subclinical mastitis in District Kasur, Punjab, Pakistan. Pakistan Journal of Zoology 51(3): 1123–1132.

Mahroug A, Mahroug I, Berra S, Hamrit S, Guelil A, Zoukel A, and Ullah S. (2023). Optical, Photocurrent, Electrical, Structural, and Morphological Properties of Magnetron Sputtered Pure and Iron-Doped Zinc Oxide Thin Films. ECS Journal of Solid State Science and Technology 12(4): 046006. DOI: 10.1149/2162-8777/accba5

Min C, Wang H, Xia F, Tang M, Li J, Hu Y and Zou M. (2022). Characteristics of Staphylococcus aureus small colony variants isolated from wound specimens of a tertiary care hospital in China. Journal of Clinical Laboratory Analysis 36(1): e24121. DOI: 10.1002/jcla.24121

Montville R and Schaffner DW. (2003). Inoculum size influences bacterial cross contamination between surfaces. Applied and Environmental Microbiology 69(12): 7188–7193. DOI: 10.1128/AEM.69.12.7188-7193.2003

Moo CL, Yang SK, Yusoff K, Ajat M, Thomas W, Abushelaibi A and Lai KS. (2020). Mechanisms of antimicrobial resistance (AMR) and alternative approaches to overcome AMR. Current Drug Discovery Technologies 17(4): 430–447. DOI: 10.2174/1570163816666190304122219

Murray PR and Zeitinger JR. (1983). Evaluation of Mueller-Hinton agar for disk diffusion susceptibility tests. Journal of Clinical Microbiology 18(5): 1269–1271. DOI: 10.1128/jcm.18.5.1269-1271.1983

Mușat V, Ibănescu M, Tutunaru D and Potecașu F. (2017). Fe-doped ZnO nanoparticles: Structural, morphological, antimicrobial and photocatalytic characterization. Advanced Materials Research 1143: 233–239. DOI: 10.4028/www.scientific.net/AMR.1143.233

Naiel MA, Enany ME, Algammal AM, Nasef SA, Abo-Eillil SAM, Bin-Jumah M and Allam AA. (2024). Antibacterial and antibiofilm activity of green-synthesized zinc oxide nanoparticles against multidrug-resistant Escherichia coli isolated from retail fish. Molecules 30(3): 768. https://doi.org/10.3390/molecules30040768

O'Neill J. (2016). Tackling drug-resistant infections globally: Final report and recommendations. Review on Antimicrobial Resistance. https://amr-review.org/sites/default/files/160518_Final%20paper_with%20cover.pdf.

Parvekar P, Palaskar J, Metgud S, Maria R and Dutta S. (2020). The minimum inhibitory concentration (MIC) and minimum bactericidal concentration (MBC) of silver nanoparticles against Staphylococcus aureus. Biomaterial Investigations in Dentistry 7(1): 105–109. DOI: 10.1080/26415275.2020.1796674

Pasieczna-Patkowska S, Cichy M and Flieger J. (2025). Application of Fourier transform infrared (FTIR) spectroscopy in characterization of green synthesized nanoparticles. Molecules 30(3): 684. https://doi.org/10.3390/molecules30030684

Rafique M, Potter RF, Ferreiro A, Wallace MA, Rahim A, Ali Malik A and Dantas G. (2020). Genomic characterization of antibiotic resistant Escherichia coli isolated from domestic chickens in Pakistan. Frontiers in Microbiology 10: 3052. https://doi.org/10.3389/fmicb.2019.03052

Rao YS, Parajuli D, Rao MS, Ramakrishna A, Ramanjaneyulu K, Mammo TW and Murali N. (2023). Effect of Fe doped and capping agent–structural, optical, luminescence, and antibacterial activity of ZnO nanoparticles. Chemical Physics Impact 7: 100270. https://doi.org/10.1016/j.chphi.2023.100270

Sardar S, Rahman AU, Khan B, Khan MA, Iqbal MK, Hasnain M and Ali Q. (2024). Vaccinium macrocarpon-based Fe-doped ZnO nanoparticles as an alternate against resistant uropathogens. BioNanoScience 14(3): 2649–2664. DOI: 10.1007/s12668-024-01576-w

Sharma N, Jandaik S, Kumar S, Chitkara M and Sandhu IS. (2016). Synthesis, characterisation and antimicrobial activity of manganese- and iron-doped zinc oxide nanoparticles. Journal of Experimental Nanoscience 11(1): 54–71. https://doi.org/10.1080/17458080.2015.1025302

Slavin YN, Asatryan RG and Sinyashin OG. (2017). Iron oxide nanoparticles: Synthesis, properties and applications. Journal of Materials Science and Technology 33(8): 993–1006.

Smith JL and Fratamico PM. (2017). Escherichia coli as a Pathogen. Foodborne Diseases 3: 189–208. https://doi.org/10.1016/B978-0-12-385007-2.00007-3

Sperber WH and Tatini SR. (1975). Interpretation of the tube coagulase test for identification of Staphylococcus aureus. Applied Microbiology 29(4): 502–505. DOI: 10.1128/am.29.4.502-505.1975

Sun L, Wang F and Wang Z. (2019). Magnetic iron-doped zinc oxide nanoparticles for improved antibacterial activity. International Journal of Nanomedicine 14: 4015–4025.

Tang KL, Caffrey NP, Nóbrega DB, Cork SC, Ronksley PE, Barkema HW and Ghali WA. (2017). Restricting the use of antibiotics in food-producing animals and its associations with antibiotic resistance in food-producing animals and human beings: A systematic review and meta-analysis. The Lancet Planetary Health 1(8): e316–e327. DOI: 10.1016/S2542-5196(17)30141-9

Van Boeckel TP, Brower C, Gilbert M, Grenfell BT, Levin SA, Robinson TP and Laxminarayan R. (2015). Global trends in antimicrobial use in food animals. Proceedings of the National Academy of Sciences of the United States of America 112(18): 5649–5654. https://doi.org/10.1073/pnas.15031411

Van Hofwegen DJ, Hovde CJ and Minnich SA. (2016). Rapid evolution of citrate utilization by Escherichia coli by direct selection requires citT and dctA. Journal of Bacteriology 198(6): 1022–1034. https://doi.org/10.1128/jb.00831-15

Vassallo J, Besinis A, Boden R, and Handy RD. (2018). The minimum inhibitory concentration (MIC) assay with Escherichia coli: An early tier in the environmental hazard assessment of nanomaterials? Ecotoxicology and Environmental Safety 162: 633–646. https://doi.org/10.1016/j.ecoenv.2018.06.085

Velazquez-Meza ME, Galarde-López M, Carrillo-Quiróz B and Alpuche-Aranda CM. (2022). Antimicrobial resistance: one health approach. Veterinary World 15(3): 743. DOI: 10.14202/vetworld.2022.743-749

Walther B, Tedin K and Lübke-Becker A. (2017). Multidrug-resistant opportunistic pathogens challenging veterinary infection control. Veterinary Microbiology 200: 71–78. DOI: 10.1016/j.vetmic.2016.05.017

Yin H, Lu Y, Chen R, Orrell-Trigg R, Gangadoo S, Chapman J, and Truong VK. (2024). Cytotoxicity and Antimicrobial Efficacy of Fe-, Co-, and Mn-Doped ZnO Nanoparticles. Molecules 29(24): 5966. https://doi.org/10.3390/molecules29245966

Zakir M, Khan M, Umar MI, Murtaza G, Ashraf M and Shamim S. (2021). Emerging Trends of Multidrug-Resistant (MDR) and Extensively Drug-Resistant (XDR) Salmonella Typhi in a Tertiary Care Hospital of Lahore, Pakistan. Micro-organisms 9(12): 2530. DOI: 10.3390/microorganisms9122 484

Zgurskaya HI and Rybenkov VV. (2020). Permeability barriers of Gram-negative pathogens. Annals of the New York Academy of Sciences 1459(1): 5–18. DOI: 10.1111/nyas.14 134

Zhang X, Li S and Li H. (2021). Antibacterial properties and mechanisms of iron-doped zinc oxide nanoparticles. Antibiotics 10(1): 58. https://doi.org/10.1016/j.colsurfa.2024.133421